Supplementary Material

Substrate binding on the APC/C occurs between the co-activator CDH1 and the processivity factor DOC1

Bettina A. Buschhorn[1,6], Georg Petzold[1,6], Marta Galova[1], Prakash Dube[2], Claudine Kraft[1,3], Franz Herzog[1,4], Holger Stark[2,5] and Jan–Michael Peters[1]

To whom correspondence should be addressed. E–mail:

Holger Stark

hstark1@gwdg.de

Jan–Michael Peters

peters@imp.ac.at

This supplement includes:

Supplementary Material and Methods

Supplementary Figures 1 to 5

Supplementary Tables 1 to 5

Supplementary References

Supplementary Material and Methods

Doc1 mutagenesis and expression. To generate "long" and "short" versions of Doc1, PCR products were generated from a *DOC1* cDNA template containing both start codons with primers 5'–ATCGATTAATACGACTCACTATAGGGCTCGAGGCCGCCACCATGGGGCAAAATA AGCGCCGTCTATAT–3' (forward primer "long") or 5'–ATCGATTAATACGACTCACTATA GGGCTCGAGGCCGCCACCATGGACCCGATTGGAATAAACAAAGT–3' (forward primer "short") and 5'–GTGCTCTCGAGTTACATCATGGATCCTTAACGTAATATAGCATCCTGG AAGAATTGTT–3' (reverse primer for both). PCR products were used as templates in coupled *in vitro* transcription/translation reactions.

N–terminal tagging of Doc1 with tdimer2. A *doc1* deletion strain was transformed with a plasmid system (kindly provided by Gwenael Rabut) allowing the exchange of the G418 selection cassette by a tagged gene version of *DOC1*. The *TDIMER2* ORF was subcloned from pGR20 (kind gift of G. Rabut) via PacI/NotI. The *DOC1* promoter, introducing an AgeI site at the 5' end, and a START codon and a PacI site (ATG TTA ATT AA) at the 3' end, was amplified from genomic DNA. NotI (plus an extra nucleotide, GCG GCC GCT ATG) and XhoI restriction sites were introduced when amplifying *DOC1* from cDNA and *DOC1* was ligated into pGR51. The resulting construct was cleaved with AgeI and NotI enzymes, and promoter and *TDIMER*2 were inserted simultaneously. The resulting plasmid was cut with AgeI and PmeI, releasing the tagged construct, which was transformed into a heterozygous *doc1* deletion strain (Mata/alpha DOC1/doc1*::KanMX*, J464) strain and positive transformants were selected on plates lacking histidine.

(tmd)phe–tRNA. (tmd)phe was obtained from Botanica GmbH, Sins, Switzerland. Alternatively, it was generated from (tmd)phe–pdCpA (generous gift from J. Brunner) and $tRNA^{SUP}_{(-pdCpA)}$ following the protocol by[1], with two major exceptions. The template for the transcription reaction was generated by PCR amplification from pTHG73 (ref. 2) using primers 5'–GCGGTCCTACTGGGATT–3' and 5'–AATTCGTAATACGACTCACTATAG–3'. The PCR product was extracted with phenol pH 7.9 and chloroform followed by ethanol precipitation. About 5 µg PCR product were used for a 100 µl transcription reaction. Secondly,

N–(4–)pentenoyl–protected (tmd)phe was deprotected with 25 mM I_2 in 1:1 tetrahydrofuran–water[3].

Gradient centrifugation and APC/C immunoprecipitation. *CDC16–HA3/CDC16–myc6* cells were lysed in a freezer mill, extracts were cleared by subsequent ultracentrifugation. The soluble fraction was diluted to a concentration of 4 mg ml^{-1} in LB50 buffer (20 mM Hepes KOH pH 8.0, 50 mM KCl, 1.5 mM MgCl2, 0.1% (v/v) NP40*,*1 mM DTT) or LB400 buffer (LB50 + 350 mM KCl), supplemented with 5% (v/v) glycerol. 4 mg of extract were separated through a 10 to 40% (v/v) glycerol gradient prepared in buffer LB50 or LB400. Centrifugation was carried out at 34000 rpm for 18 h at 4°C in a Beckman SW40 rotor in a Beckman Optima MAX ultracentrifuge (Beckman Coulter). Gradients were fractionated into 400 µl aliquots using an ISCO fractionator. APC/C was immunoprecipitated in each fraction using 12CA5 (HA) antibody beads. Beads were washed with LB50 containing 10% (v/v) glycerol. Proteins were eluted with 100 mM glycine pH 2.2 and analyzed by western blotting. Apc1–myc/Apc1–HA coimmunoprecipitations were carried out as described[4]. Briefly, 12CA5 and 9E10 antibodies were bound to protein A sepharose (Biorad) and GammaBind G sepharose (GE Healthcare) beads, respectively. Extracts were prepared in buffer (50 mM Tris pH 7.5, 50 mM NaCl, 10% (v/v) glycerol, 0.2% (v/v) Triton X–100, 1 mM DTT) by bead beating. 10 µl beads each were incubated with cleared lysates containing 2 mg protein for 90 min at 4°C. Beads were washed with buffer, and bound proteins were eluted with 15 µl 100 mM glycine pH 2.2.

Antibodies. Antibodies against Apc1, Cdc16, Cdc23, Doc1 and Apc11 were raised by immunizing rabbits with peptides coupled to Keyhole Limpet Hemocyanin (Apc1: CDDERSSNGSDISDPTAYLEDKKDIDDHYG; Cdc16: CALRKGGHDSKTGSNNADDDFDAD; Cdc23: SLADESPLRNKQGVPKQMFC; Doc1: CSNEPHQDTHEWAQTLPETNNV; Apc11: CVDFDEPIRQNTDNPIGRQQV). 9E10 and 12CA5 antibodies were used for immunoprecipitation and immunodetection of the myc– and HA–epitopes, respectively.

Cryo–Negative Stain Electron microscopy. Purified APC/C or APC/C–antibody complexes were adsorbed to a thin film of carbon and then transferred to an electron microscopic grid

covered with a perforated carbon film. The bound APC/C particles were stained with 2% (w/v) uranyl formate, blotted and air dried for ~1 min at room temperature. For cryo–negative staining the grids were subsequently plunged into liquid nitrogen. Images were recorded at a magnification of 155,000x on a 4k x 4k CCD camera (TVIPS GmbH) using two–fold pixel binning (1.8 Å per pixel) in a Philips CM200 FEG electron microscope (Philips/FEI) operated at 160 kV acceleration voltage. APC/C–antibody complexes were imaged at room temperature using the same magnification.

Image Processing. Particle images (200 x 200 pixel) were selected using the semiautomated software boxer as part of the Eman package. Images were coarsened by a factor of two resulting in 100 x 100 pixels per image with a sampling of ~3.8 Å per pixel. After CTF correction[5], images were aligned using an exhaustive multi–reference alignment based on re–sampling to polar coordinates[6]. To obtain the initial 3D reconstructions we made use of random–conical–tilt imaging and weighted averaging of 3D volumes[7]. Characteristic views were obtained by averaging after multivariate statistical analysis and classification[8]. Angular reconstitution[9] was used to determine the relative orientations of the projection images prior to computing the 3D reconstruction. 3D structures were visualized with the software AmiraDev 2.3 (TGS Europe, Merignac Cedex).

Supplementary Figures

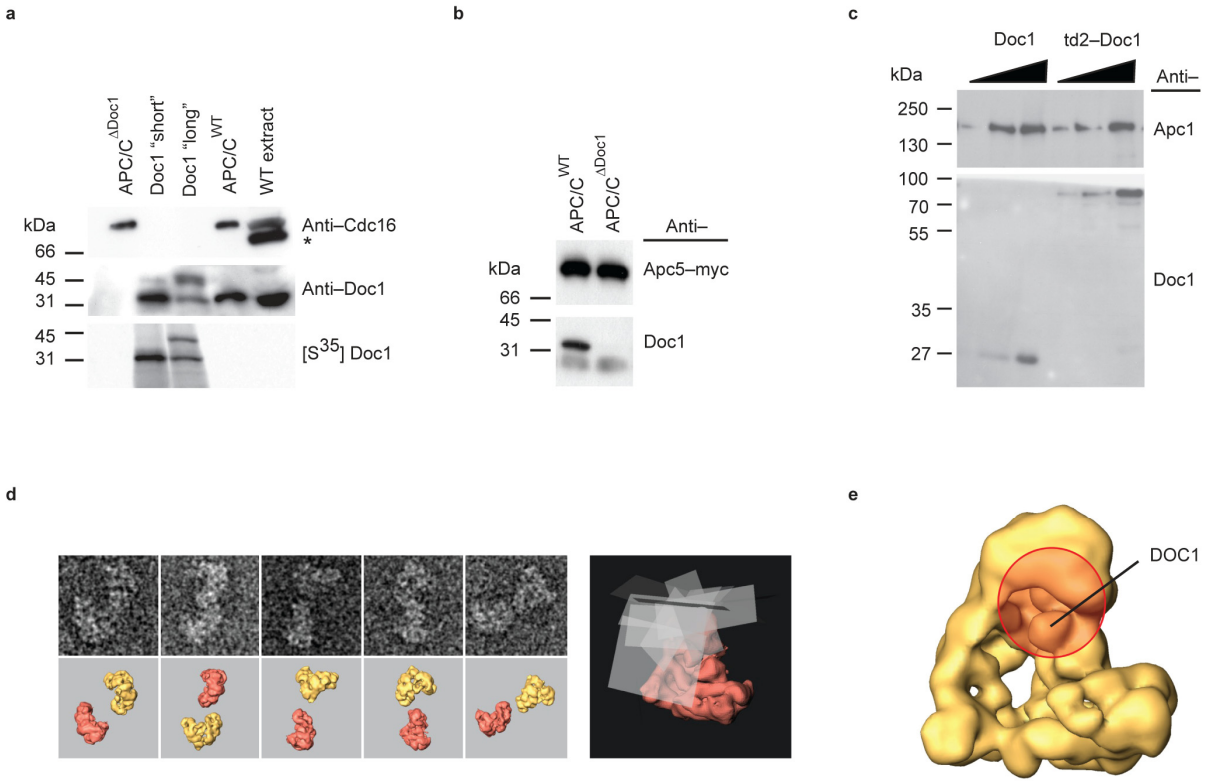

Supplementary Figure 1 Doc1 characterization and localization using tdimer2 tagging and antibody labeling. (**a**) Yeast cell extracts only contained a 30 kDa version of the Doc1 subunit, which can be co–purified with wild type APC/C and is absent in APC/C$^{\Delta Doc1}$. *In vitro* translated (IVT) products of either the short or the long *DOC1* ORF version serve as reference. The asterisk marks the TAP–tag recognized by the Cdc16 antibody in the cell extract. (**b**) Doc1 is absent in *doc1* deletions strains. Both wild type and *doc1* deletion strains were used to TAP–tag purify APC/C via the Apc4 subunit. (**c**) N–terminal tdimer2–labeling of yeast Doc1. Western blot analysis of TAP–tag purified APC/C shows that Doc1 labeling results in a mobility shift from ~ 30 to ~ 80 kDa. (**d**) Localization of human DOC1 protein by antibody labeling. The orientation of APC/C within the APC/C–antibody complex was evaluated based on the known APC/C structure. Rectangles were modeled to the APC/C 3D structure at the respective binding sites of the antibody and the binding site was determined as the main crossing 3D area of all rectangles[10]. (**e**) The antibody epitope is marked on the surface of the human APC/C 3D model and labeling

accuracy is indicated by the size of the area. A structurally similar domain compared to yeast APC/C Doc1 is situated within this area, indicating a conserved localization of the Doc1 subunit in yeast and human APC/C.

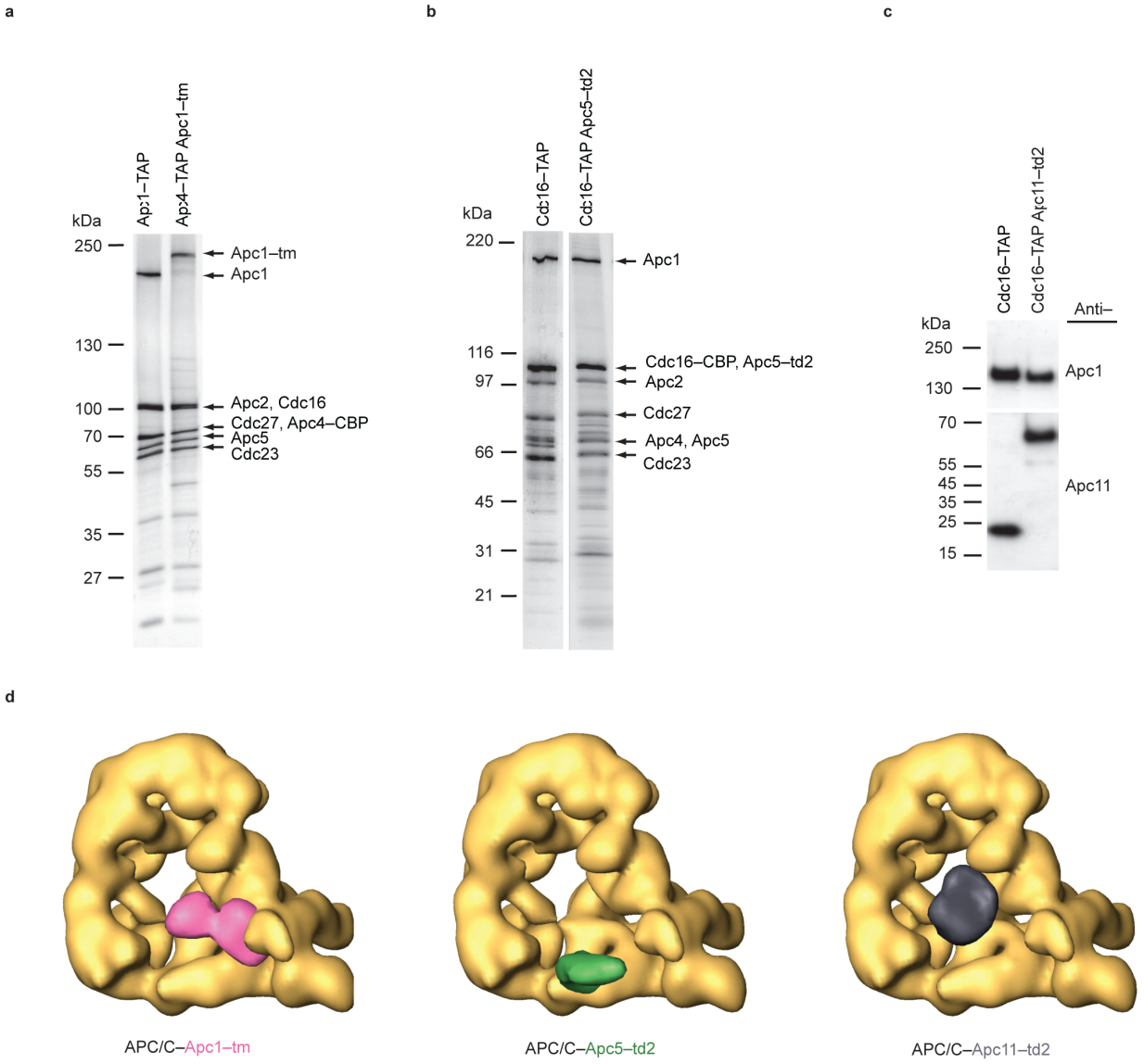

Supplementary Figure 2 Yeast APC/C subunit localization using td2–labeling. (**a**) Subunit labeling of the yeast Apc1 subunit. Apc1 was tagged with a tmonomer–tag and TAP–tag purified via Apc4. Apc1 undergoes a mobility shift upon tmonomer labeling in the silver stained SDS–PAGE. Apc4–CBP indicates calmodulin binding protein remaining on Apc4 after TEV cleavage. (**b**) SDS–PAGE of Apc5–tdimer2 labeled APC/C TAP–tag purified via the Cdc16 subunit. (**c**) Western blot analysis of tdimer2 labeled Apc11. Yeast APC/C complexes were TAP–tag purified via the Cdc16 subunit. (**d**) Yeast APC/C 3D models indicating subunit localization of Apc1, Apc5 and Apc11 by colored extra density elements representing the tdimer2 label.

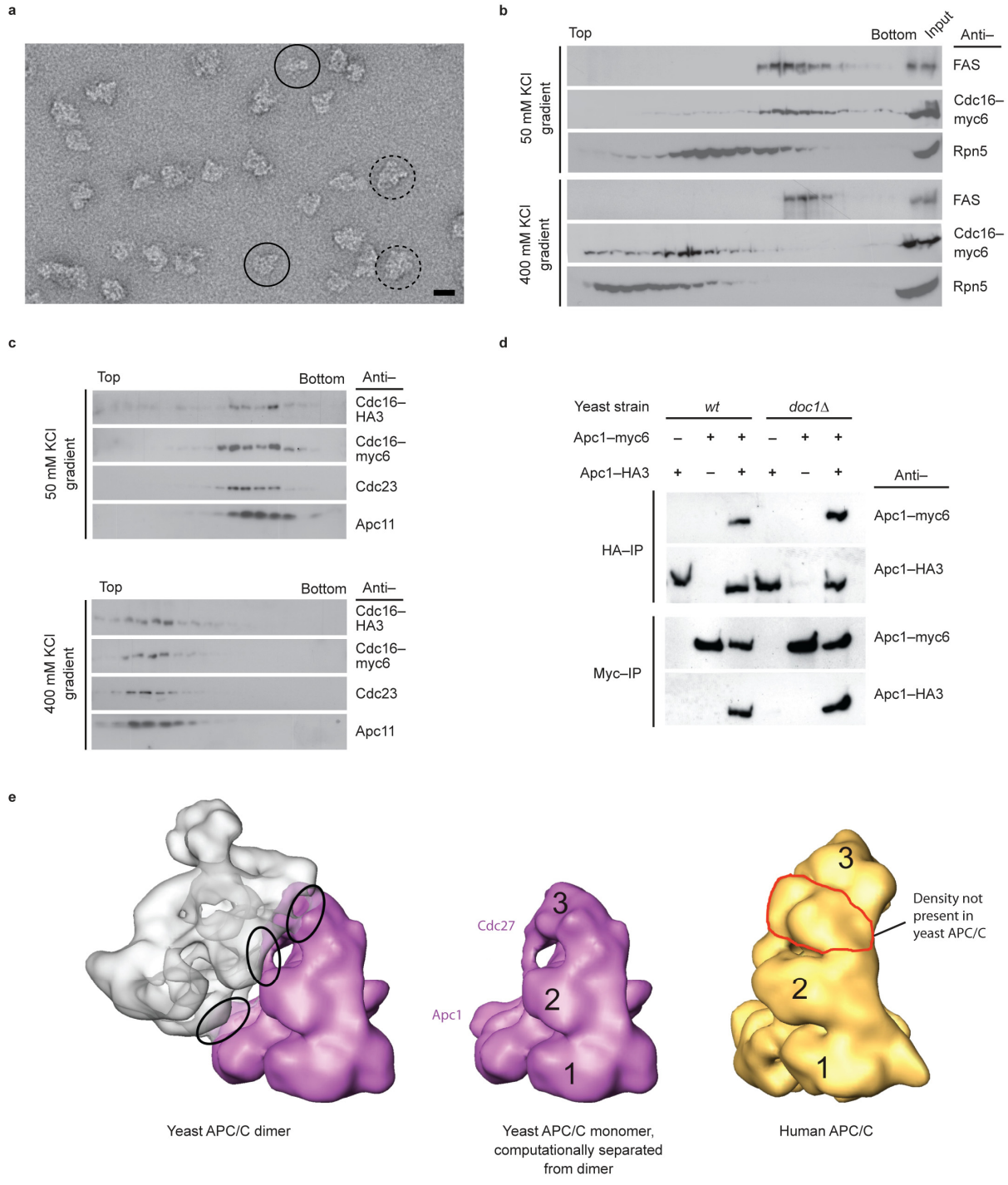

Supplementary Figure 3 Analysis of yeast APC/C dimers. (**a**) Electron microscopic raw images of cryo–negative stained yeast APC/C monomers and dimers. Continuous circles exemplify monomeric, dashed circles dimeric yeast APC/C. (**b**) Yeast extracts primarily contain dimeric APC/C, which can be dissociated into monomers applying high salt conditions. Fractions of the

gradients were analyzed by Western blot. Fatty acid synthase (41 S) and the 26 S proteasome subunit Rpn5 (ref. 11) serve as sedimentation markers. (**c**) Dimeric APC/C dissociates into monomers under high–salt conditions. Extracts from a diploid *CDC16–HA2/CDC16–myc6* yeast strain were used for glycerol density gradient centrifugation in the presence of either high or low salt concentrations. After gradient fractionation, APC/C was immunoprecipitated with HA antibodies from each fraction and analyzed by Western blotting. Under both conditions, Cdc16–HA2 co–immunoprecipitated Cdc16–myc6, demonstrating that monomeric yeast APC/C contains at least two copies of the Cdc16 subunit. (**d**) Self association of Apc1 is not impaired in the absence of Doc1. Wild type or *doc1Δ* diploid yeast strains carrying indicated epitope–tagged Apc1 versions were used for immunoprecipitation experiments. Apc1 is believed to be present as one copy within monomeric APC/C[12,13]. Apc1–HA3 could co–immunoprecipitate Apc1–myc9 (and vice versa) when co–expressed in presence and absence of Doc1, which indicates that APC/C dimerization does not depend on Doc1. (**e**) Yeast APC/C dimer interface involves bulky domains located on the back side of the TPR–rich arc lamp domain, labeled 2 and 3. Due to structural resemblance, similar domains could be identified and allocated in human APC/C. Compared to yeast APC/C the human 3D model carries a significant extra mass inserted within the dimer interface between domain 2 and 3, resulting in a more extended appearance of the arc lamp domain. This insertion might prevent dimerization of human APC/C.

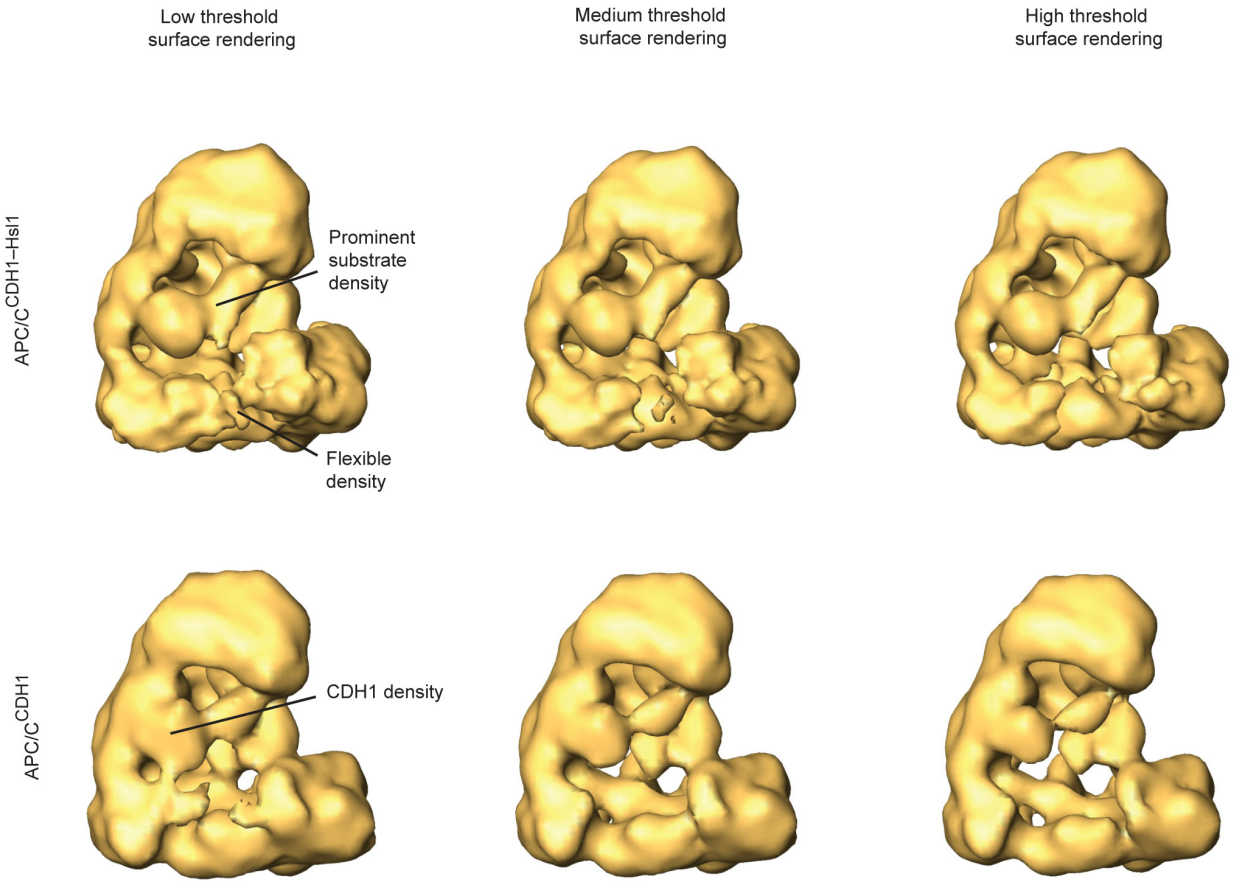

Supplementary Figure 4 $APC^{CDH1–Hsl1}$ and APC^{CDH1} depicted with different surface rendering thresholds. In the 3D model of $APC^{CDH1–Hsl1}$ a second extra density could be resolved near the platform domain. This second density disappears upon increase of the threshold parameter for surface rendering, indicating a structural heterogeneity in the platform region among $APC^{CDH1–Hsl1}$ complexes contained in the dataset. The two extra densities in the $APC^{CDH1–Hsl1}$ 3D model might represent two distinct domains of the bound His–Flag–td2–$Hsl1^{667–872}$ molecule. Importantly, using high threshold parameter settings, the density intercalated between CDH1 and DOC1 remained appreciable compared to APC^{CDH1}.

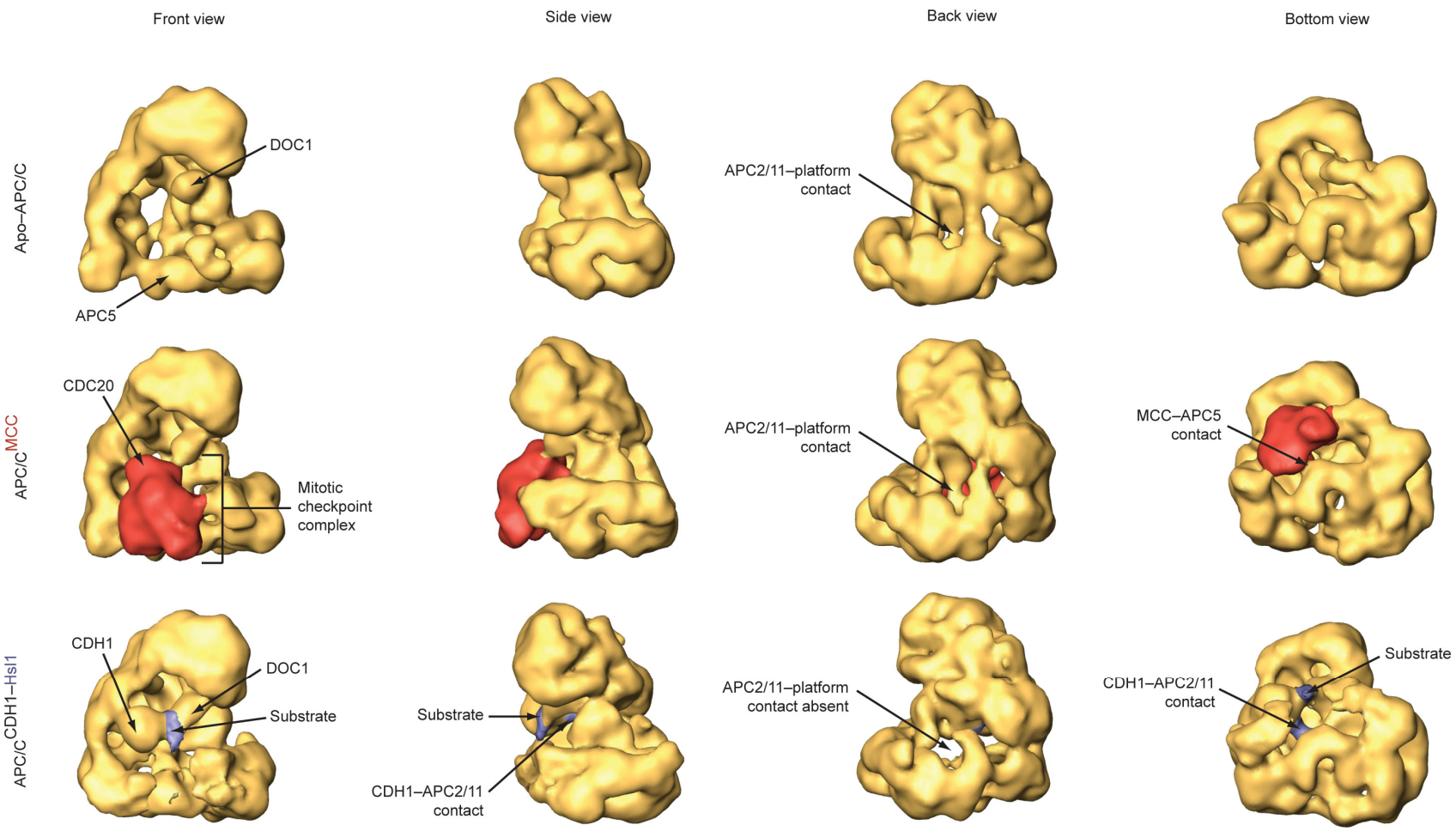

Supplementary Figure 5 Comparison of human apo–APC/C, APC/C^{MCC} and APC/C$^{CDH1–Hsl1}$.

Supplementary Figure 5 Comparison of human apo–APC/C, APC/C^{MCC} and APC/$C^{CDH1–Hsl1}$. The three different complexes are shown in their front, side, back and bottom view orientation. As reported previously[10], the mitotic checkpoint complex is inserted into the central cavity located at the front side of the platform domain. In the APC/C^{MCC} 3D model, the position of the co–activator density (CDC20) is changed compared to the position of CDH1 in the APC/C structure bound to a substrate molecule. These orientational differences might contribute to decreased substrate recognition as shown for APC/C^{MCC} (ref. 10) by disrupting the bipartite substrate receptor. In apo–APC/C, the APC2–APC11 module contacts an unknown subunit located in the platform domain, which is also observed in the APC/C^{MCC} structure (back view orientation). Interestingly, in the 3D model of APC/$C^{CDH1–Hsl1}$ this connection to the platform is absent and instead, APC2–APC11 forms a new contact to the co–activator density (back and bottom view orientation).

Supplementary Tables

Supplementary Table 1 Doc1 sites exchanged with photo–activatable amino acids.

Site of incorporation	Site in "long" Doc1	Location of site in structure
Arg37	Arg70	Back side
His67	His100	N–terminal helix
Gln71	Gln104	N–terminal helix
Lys91	Lys124	Front side
Lys96	Lys129	Front side
Leu97	Leu130	Front side
Phe103	Phe136	Front side
Asp110	Asp143	Front side
Asp116	Asp149	Front side
Ser128	Ser161	C–terminal region
Lys129	Lys162	C–terminal region
Arg130	Arg163	C–terminal region
Glu146	Glu179	Back side
Lys154	Lys187	Front side
Arg182	Arg215	Back side
Arg199	Arg232	Front side
Asn205	Asn238	Processivity loop
His206	His239	Processivity loop
Glu207	Glu240	Processivity loop
Asn208	Asn241	Processivity loop
Lys210	Lys243	Processivity loop
Asp211	Asp244	Processivity loop
Glu239	Glu272	IR–tail
Phe244	Phe277	IR–tail

For easier comparison with previous studies[14], corresponding positions in the "long" Doc1 construct are provided. Regions within Doc1 were classified based on orientation in Figure 1e.

Supplementary Table 2 List of all Doc1 interactions identified by photo–crosslinking.

site of incorporation	site in "long" Doc1	interaction partner
Ser128	Ser161	Apc1 (+++)
		Cdc16 (+)
Lys129	Lys162	Cdc16 (+++)
		Apc1 (+)
Lys154	Lys187	Apc1 (+++)
Arg182	Arg215	Cdc16 (+++)
Asn205	Asn238	Apc1 (+)
Phe244	Phe277	Cdc27 (+++)

+++ abundant, + less abundant crosslinks. Listed crosslinks were observed in at least five experiments.

Supplementary Table 3 Statistics on EM image analysis.

Sample	Number of particles	Resolution
Yeast APC/C monomer	55434	25 Å
Yeast APC/C dimer	1271	35 Å
Human APC/C$^{CDH1–Hsl1}$	14813	28 Å
Human APC/C^{CDH1}	17075	27 Å
Yeast APC/C$^{\Delta Swm1}$	6256	33 Å
Yeast APC/C$^{\Delta Doc1}$	28383	30 Å
Yeast APC/C–Apc1–tmonomer	10474	30 Å
Yeast APC/C–Apc2–tdimer2	12171	32 Å
Yeast APC/C–Apc3–tdimer2	11767	39 Å
Yeast APC/C–Apc5–tdimer2	10291	35 Å
Yeast APC/C–Apc6–tdimer2	14421	38 Å
Yeast APC/C–Apc11–tdimer2	13480	32 Å
Yeast APC/C–Swm1–tdimer2	6273	34 Å
Yeast APC/C–Doc1–tdimer2	9228	30 Å

Supplementary Table 4 Summary of subunit localization experiments. Methods used in this and previous studies for the localization of different subunits and interacting proteins in the 3D structure of the APC/C from different species.

Subunit	**Subunit deletion**	**td2 tagging**	**Antibody labeling**	**Recombinant protein addition**
Species	*S. cerevisiae*	*S. cerevisiae*	*H. sapiens, X. laevis*	*H. sapiens, X. laevis*
Apc1	–	1	2	–
Apc2	–	–	2,3	–
Cdc27	–	1	2	–
Apc4	–	–	2	–
Apc5	–	1	2	–
Cdc16	–	1	–	–
Cdc23	–	–	–	–
Apc7	n.i.	n.i.	–	–
Apc9	–	–	n.i.	n.i.
Doc1	1	1	1	–
Apc11	–	1	–	–
Apc16	n.i.	n.i.	4	–
Mnd2	–	–	n.i.	n.i.
CDH1	–	–	–	1,2,3
CDC20	–	–	–	2
Swm1/Apc13	1	1	–	–
BUBR1	–	–	2	–
Hsl1	–	–	–	1

Indicated sources are: [1] this study; [2] (ref. 10); [3] (ref. 12); [4] (ref. 15); n.i. not identified.

Supplementary Table 5 Yeast strains used in this study.

Strain	Relevant genotype	background	Source
K6201	*MATa APC1–ha3::HIS3*	W303	(ref. 4)
K6202	*MATalpha APC1–myc6::HIS3*	W303	(ref. 4)
K6203/YWZ197	*MATa/MATalpha,CDC16–myc6::URA3/CDC16–ha3::URA3*	W303	Gift from Kim Nasmyth
Z1850	*MATalpha CDC16TAP::KlTRP1 pep4::URA3*	W303	(ref. 16)
Z2304	*Matalpha, CDC16–Tap::KlTRP1, swm1::KanMX4, pep4::URA3*	W303	Gift from Kim Nasmyth
J9	*MATa APC4–TAP::KlTRP1*	W303	this study
J180	*MATa APC4–TAP::KlTRP1 doc1::KanMX*	W303	this study
J182	*MATa APC4–TAP::KlTRP1 APC1–myc18::HIS3 doc1::KanMX*	W303	this study
J187	*MATa APC4–TAP::KlTRP1 APC5–myc9::KlTRP1 doc1::KanMX*	W303	this study
J189	*MATa APC4–TAP::KlTRP1 APC2–myc9::TRP1 doc1::KanMX*	W303	this study
J220	*MATa doc1::KanMX*	W303	this study
J235	*MATa APC4–TAP::TRP1 CDC16–myc6::URA3 doc1::KanMX*	W303	this study

J266	*MATa APC4–TAP::KlTRP1 CDC27–myc9::TRP1 doc1::KanMX*	W303	this study
J319	*MATalpha APC4–TAP::KlTRP1 pep4::URA3*	W303	this study
J320	*MATa CDC16TAP::KlTRP1 doc1::KanMX pep4::URA3*	W303	this study
J323	*MATa APC4–TAP::KlTRP1 doc1::KanMX pep4::URA3*	W303	this study
J325	*MATa/alpha APC1–ha3::HIS3/APC1–myc6::HIS3*	W303	this study
J326	*MATa APC1–ha3::HIS3 doc1::KanMX*	W303	this study
J327	*MATalpha APC1–myc6::HIS3 doc1::KanMX*	W303	this study
J328	*MATa/alpha APC1–ha3::HIS3/APC1–myc6::HIS3 doc1::KanMX*	W303	this study
J329	*MATa APC4–TAP::KlTRP1 APC1–tmono::SpHIS5 pep4::URA3*	W303	this study
J347	*MATalpha CDC16TAP::KlTRP1 pep4::URA3 APC4–tdimer2::SpHIS5*	W303	this study
J376	*MATalpha CDC16TAP::KlTRP1 CDC27–tdimer2::spHIS5 pep4::URA3*	W303	this study
J378	*MATa APC4–TAP::KlTRP1*	W303	this study

	CDC16–tdimer2::spHIS5 pep4::URA3		
J380	*MATalpha CDC16–TAP::KlTRP1 APC5–tdimer2::SpHIS5 pep4::URA3*	W303	this study
J406	*MATa CDC16TAP::KlTRP1 pep4::URA3 CDC26–tdimer2::SpHIS5*	W303	this study
J407	*MATa CDC16TAP::KlTRP1 pep4::URA3 MND2–tdimer2::SpHIS5*	W303	this study
J408	*MATa CDC16TAP::KlTRP1 pep4::URA3 APC2–tdimer2::SpHIS5*	W303	this study
J422	*MATa CDC16–TAP::KlTRP1 pep4::URA3 APC11–tdimer2::SpHIS5*	W303	this study
J428	*MATa CDC16TAP::KlTRP1, pep4::URA3 SWM1–tdimer2:sp:HIS5*	W303	this study
J464	*MATa/MATalpha doc1::KanMX/DOC1*	W303	this study
J475	*MATalpha, N–tdimer2–DOC1::HIS3 CDC16–TAP::KlTRP1, pep4::URA3*	W303	this study
J477	*Matalpha, mnd2::KanMX CDC16–TAP::KlTRP1, pep4::URA3*	W303	this study
J497	*Mata,*	W303	this study

	cdc26::KIURA3,CDC16–TAP::KlTRP1		
BY4741	*hi3D1 leu2Δ0 met15ΔD0 ura3Δ0*	S288C	Euroscarf
yCK350	*BY4741 doc1::KanMX*	S288C	this study

All strains used in this study are derivatives of K699 (*MATa ade2–1 trp1–1 can1–100 leu2–3,112 his3–11,15 ura3–1, GAL psi*) and K700 (*MATalpha ade2–1 trp1–1 can1–100 leu2–3,112 his3–11,15 ura3–1, GAL psi*) with the exception of the strains used for spotting experiments which are derivatives of S288C (*hi3D1 leu2D0 met15D0 ura3D0 doc1::KanMX*). *Kl* denotes the *TRP1* gene from *Klyveromyces lactis*, *Sp* the *HIS5* gene from *Schizosaccharomyces pombe*.

Supplementary References

1. Graf, R., Brunner, B., Dobberstein, B. & Martoglio, B. Probing the molecular environment of proteins by site-specific photocrosslinking. in *Cell Biology, A Laboratory Handbook.*, Vol. 4 (ed. In Celis, J.E.) 495-502 (Academic Press, San Diego, CA, 1998).
2. Saks, M.E. & Sampson, J.R. Variant minihelix RNAs reveal sequence-specific recognition of the helical tRNA(Ser) acceptor stem by E.coli seryl-tRNA synthetase. *Embo J* **15**, 2843-9 (1996).
3. Lodder, M., Wang, B. & Hecht, S.M. The N-pentenoyl protecting group for aminoacyl-tRNAs. *Methods* **36**, 245-51 (2005).
4. Zachariae, W., Shin, T.H., Galova, M., Obermaier, B. & Nasmyth, K. Identification of subunits of the anaphase-promoting complex of Saccharomyces cerevisiae. *Science* **274**, 1201-4. (1996).
5. Sander, B., Golas, M.M. & Stark, H. Automatic CTF correction for single particles based upon multivariate statistical analysis of individual power spectra. *J Struct Biol* **142**, 392-401 (2003).
6. Sander, B., Golas, M.M. & Stark, H. Corrim-based alignment for improved speed in single-particle image processing. *J Struct Biol* **143**, 219-28 (2003).
7. Sander, B., Golas, M.M., Luhrmann, R. & Stark, H. An approach for de novo structure determination of dynamic molecular assemblies by electron cryomicroscopy. *Structure* **18**, 667-76.
8. van Heel, M. Multivariate statistical classification of noisy images (randomly oriented biological macromolecules). *Ultramicroscopy* **13**, 165-83 (1984).
9. Van Heel, M. Angular reconstitution: a posteriori assignment of projection directions for 3D reconstruction. *Ultramicroscopy* **21**, 111-23 (1987).
10. Herzog, F. et al. Structure of the anaphase-promoting complex/cyclosome interacting with a mitotic checkpoint complex. *Science* **323**, 1477-81 (2009).
11. Glickman, M.H. et al. A subcomplex of the proteasome regulatory particle required for ubiquitin-conjugate degradation and related to the COP9-signalosome and eIF3. *Cell* **94**, 615-23 (1998).

12. Dube, P. et al. Localization of the coactivator Cdh1 and the cullin subunit Apc2 in a cryo-electron microscopy model of vertebrate APC/C. *Mol Cell* **20**, 867-79 (2005).
13. Passmore, L.A. et al. Structural analysis of the anaphase-promoting complex reveals multiple active sites and insights into polyubiquitylation. *Mol Cell* **20**, 855-66 (2005).
14. Carroll, C.W., Enquist-Newman, M. & Morgan, D.O. The APC subunit Doc1 promotes recognition of the substrate destruction box. *Curr Biol* **15**, 11-8 (2005).
15. Hutchins, J.R. et al. Systematic analysis of human protein complexes identifies chromosome segregation proteins. *Science* **328**, 593-9 (2010).
16. Schwickart, M. et al. Swm1/Apc13 is an evolutionarily conserved subunit of the anaphase-promoting complex stabilizing the association of Cdc16 and Cdc27. *Mol Cell Biol* **24**, 3562-76 (2004).